Title

Hydrogel Beads for the Detection of Disease Biomarkers in Resource-Limited Settings

Author

Pandolfi, Paula

Publication Date

2022

Peer reviewed|Thesis/dissertation

UNIVERSITY OF CALIFORNIA

Los Angeles

Hydrogel Beads for the Detection of Disease Biomarkers in Resource-Limited Settings

A thesis submitted in partial satisfaction of the

requirements for the degree Master of Science

in Bioengineering

by

Paula Pandolfi

2022

ABTRACT OF THE THESIS

Hydrogel beads for the detection of disease biomarkers in resource-limited settings

by

Paula Pandolfi

Master of Science in Bioengineering

University of California, Los Angeles, 2022

Professor Daniel. T. Kamei, Chair

Point-of-care (POC) diagnostics are easy-to-use, low-cost devices that can rapidly detect a biomarker of interest without the need for highly trained personnel or expensive equipment. In resource-limited settings, POC testing is often the only viable option for patients, which highlights the importance of developing sensitive technologies for early disease detection and monitoring of treatment methods.

Hydrogels are flexible 3D structures made with crosslinked hydrophilic components that absorb large amounts of water. These systems are sensitive to different chemical or physical stimuli, and the magnitude of their response is usually directly proportional to the magnitude of the applied external stimuli. In the diagnostics field, hydrogels are mostly being used for enzyme detection and immunodiagnostics. For these applications, the biomarker acts as a signal that

triggers a volume, color, or state change of the hydrogel, an example of the latter being a gel-sol transition or vice versa. This technology often requires the chemical modification of at least one of the main hydrogel components so that the system is specific towards the molecule of interest. Accordingly, these devices need to be manufactured in a laboratory setting with complex equipment and often expensive reagents, and they also require personnel with extensive knowledge and experience to conduct the assay and its analysis. Thus, it would be desirable to design a hydrogel system that is responsive to the presence of the biomarker of interest without the need for chemical modification of the reagents to design a robust, POC-friendly device that can be manufactured in all parts of the world.

To develop this system, we focused on calcium alginate dextran hydrogels beads for the detection of abnormal concentrations of ions, such as bicarbonate and phosphate, in patient samples. This system can be synthesized by a simple ionic crosslinking method based solely on the complexation of the oppositely charged species, i.e., alginate and calcium, which comprise the gel matrix. For disease detection, we took advantage of a calcium depletion mechanism based on the reaction of the biomarkers of interest with the divalent calcium cation in the calcium alginate gel matrix. The timeframe for hydrogel degradation was therefore correlated with the sample's ion concentration, making our POC device semi-quantitative.

To our knowledge, this is the first demonstration of the use of nonionic polymers to improve the morphology of calcium alginate hydrogel beads using a simple processing method that involves minimal labor, equipment, and reagents. The simplified bead synthesis protocol combined with a user-friendly device that we developed allows for the rapid detection of high serum bicarbonate or urine phosphate levels at the POC.

The thesis of Paula Pandolfi is approved.

Benjamin M. Wu

Wentai Liu

Daniel T. Kamei, Committee Chair

University of California, Los Angeles

2022

TABLE OF CONTENTS

TABLE OF FIGURES

ACKNOWLEDGMENTS

First, I would like to thank my mentor Dr. Kamei. He is the best professor I've ever had and his passion for teaching and bioengineering is contagious. BE C201 was one of my favorite courses of all time. The topics were fascinating but what really made a difference for me was the way Dr. Kamei encouraged us to learn for ourselves, more so than for a grade. Because of this I got to immerse myself in the class in a way I hadn't experienced before and now that is how I approach every learning experience I am presented with. As a research mentor the same applies. I learnt to work hard and give it all, for myself. Not trying to impress anyone or have a perfect curriculum, just focusing on growing and enjoying every step I take towards becoming the scientist I want to be.

I also wanted to thank Cecilia Zhang, who worked with me throughout my entire time here. I often felt overwhelmed and anxious, which got in the way of my work sometimes, but instead of being upset about it, as any team member would have the right to be, she helped me through every single one of those difficult times with patience and understanding. She helped me trust my work and my skills as a researcher, but most importantly she taught me how to take things one step at a time, trusting that if I did my best, it was enough.

Yui Nadalin, who also worked closely with Cecilia and I during our project, was also a very important person in my journey. It was a pleasure being her mentor this past year. She is a dedicated and passionate student, and she gave this project her all time and time again.

The rest of the Kamei Lab graduate students, "The Overgrads", were a significant source of support and motivation daily. Their good-nature and warmth made me feel at home every day in the office, which is amazing considering my actual home is thousands of miles away.

I also wanted to thank those in my personal life. My boyfriend, Juan, who is a huge source of inspiration to me. He was there in every single study session and at the end of every intense workday, making me laugh and keeping me company, helping me navigate the challenges I came across with nothing but love and support. I feel as if I could take on the whole world if I have him by my side.

I want to thank my dad, who has been my role model for as long as I can remember. He has taught me how to love and care for those around me, with his extreme generosity and wonderful approach to life. He is the wisest and smartest person I know, and I am lucky enough to have him as my guide and friend. Him and my late grandmother, Beatriz, are the reason I can give love away so freely and with my entire heart, and I wouldn't like to live my life any other way. My grandmother still inspires me constantly and her warmth and company are with me every day even if she is not.

I want to thank my mom as well, who held my hand during my most difficult times, and understood me when I needed it the most. At my worst, she was there guiding me every step of the way, and I will always be grateful for that. She has this fire inside of her that is visible from a mile away and inspires everyone around her. She is such a strong and capable woman, who accomplishes anything she sets her mind to and more. I would also like to mention my late aunt, Jimena, who was a loving and vibrant force in my family and was taken from us too soon. I think about her and miss her every day.

Lastly, I would like to thank my cat, Cuba, and my dog Lana. The fluffiest and best friends I could ever ask for.

Chapter 2 is a version of P. Pandolfi, H. Zhang, Y. Nadalin, M. Prasetyo, A. Toubian, B.M. Wu, and D.T. Kamei. *Degradation of Hydrogel Beads for the Detection of Serum Bicarbonate*

Levels for the Diagnosis of Metabolic Alkalosis at the Point of Care, which is in preparation for submission. D. T. Kamei was the director of research for this article. This project was supported by UCLA funds.

Chapter 1: Motivation and Background

1.1 Introduction: Alginate as a biomaterial

Alginate is an anionic polysaccharide extracted from brown algae. It is a linear block copolymer composed of (1,4)-linked β-d-mannuronate (M) and α-l-guluronate (G) residues. Different species of alginate are composed of different blocks, as the G and M residues can be found in many forms, such as GGGGGG, MMMMMM or GMGMGM polymer blocks, as seen in Figure 1-1 below. Accordingly, the M/G ratio varies depending on the material's source and thus different alginates can be extracted for specific purposes.[1]

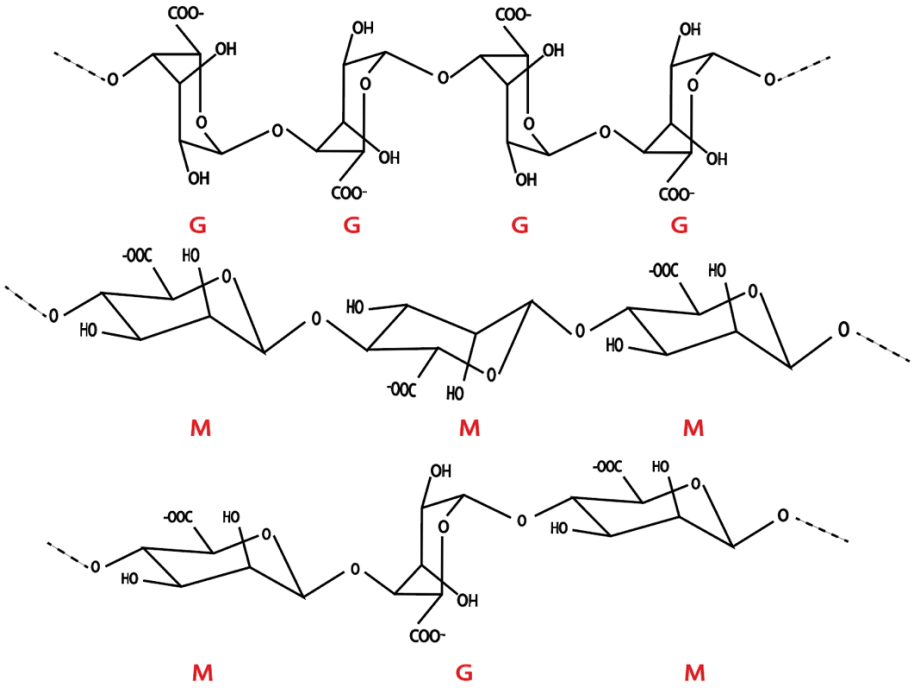

Figure 1-1. Different alginate structures. Chair conformation of alginate polysaccharide made with varying compositions of G and M polymer blocks.

Nevertheless, all alginates are biocompatible, have low toxicity, and are inexpensive which is why they are currently being used in a wide range of applications by different industries. In the dentistry field, it is used for molding, casting, and impressions.[2] It is also widely used in the textile industry as an anti-flammable and waterproof material.[3] In the food industry, alginate is used as a supplement, thickening, or stabilizing agent, and sometimes even as a coating material to increase produce shelf life due to its natural antimicrobial and antiviral properties.[4] In the pharmaceutical industry, it can be used to aid in the controlled release of small molecules for efficient and long-term drug delivery.[5] Additionally, alginate is present in many drug formulations in combination with aluminum hydroxide and magnesium carbonate to treat stomach ulcers, gastroesophageal reflux disease, heartburn, and other similar disorders.[6]

1.2 Calcium alginate hydrogels and their applications

The G blocks in alginate can bind to positively charged electrolyte species such as divalent cations. Examples of divalent cations used for binding alginate include magnesium, copper, and calcium. When the materials are incubated together, there is an instantaneous gel formation based on the electrostatic attractive interactions between the negatively charged alginate polymer and the metal cations. This method of synthesizing hydrogels is referred to as ionic crosslinking. This technique is particularly attractive as it requires minimal equipment and labor.[1]

The resulting gel matrix is described by the “egg box” model, where ions are trapped in between the anionic polymer strands. Although this theory hasn’t been proved due to the poor diffraction pattern of alginate strands, it is the most widely accepted hypothesis for calcium alginate hydrogel formation as the “egg-box” conformation is seen in other similar types of gels, such as acid gels, where better diffraction patterns make their conformations detectable. This

model describes the binding between the two oppositely charged species, alginate and calcium.[7] This interaction is depicted in Figure 1-2, where a total of four G blocks interact with one calcium cation, creating a sort of pocket that entraps the metal. Thus, the gel matrix is mostly comprised of alginate strands which are complexed together by the positive electrolyte.

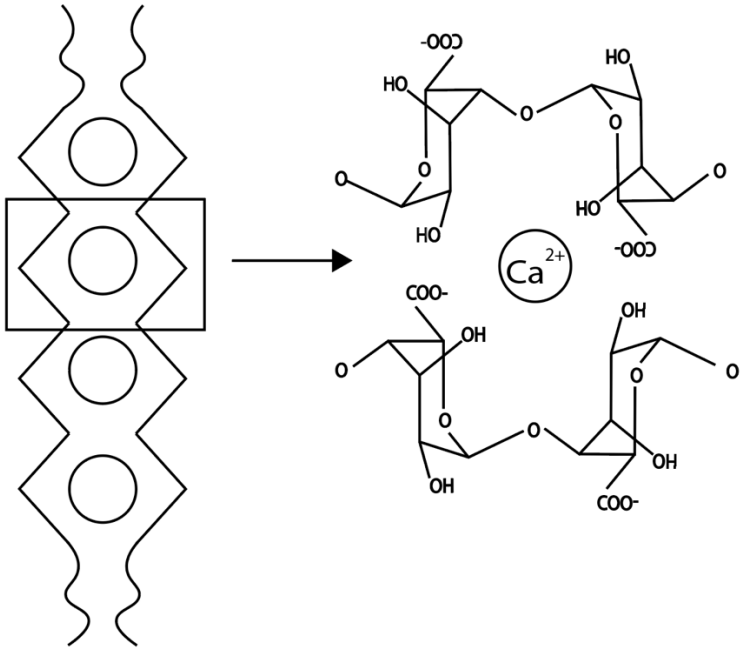

Figure 1-2. Schematic depicting the "egg box" model. The G blocks in the alginate strand, represented as solid circles, interact with the divalent calcium cations to entrap them in pockets.

In the biomedical field, most approaches take advantage of the simplicity of ionic crosslinking but have key differences in the way the reagents are dispensed and incubated together and in the way different equipment are used. One example is the application of calcium alginate gel structures to create wound dressings with innate healing properties, which takes advantage of alginate's antimicrobial properties. In this application, calcium alginate fibers are often created by a wet spinning technique where a highly concentrated alginate solution is extruded in a gelation

bath made of water and a calcium salt.[8] Another example is the formation of calcium alginate microspheres or nanospheres for small molecule or protein delivery. For this purpose, a microfluidic device is typically used to create calcium alginate hydrogel droplets in the micron and nanometer length scales. The oil-in-water (O/W), water-in-oil (W/O), or double emulsion system was developed for this specific purpose. Alginate gels synthesized in this manner can also be used to entrap living cells for a variety of different purposes such as creating scaffolds for tissue regeneration approaches that involve cell isolation and/or transplantation.[9]

1.3 Concluding remarks and thesis overview

Calcium alginate gels are very sensitive to stimuli as alginate has a relatively weak interaction with calcium when compared to other metals. Accordingly, there is potential to design a robust, rapid, and inexpensive diagnostic that involves chelating calcium from the gels. Our diagnostic was based on the degradation of hydrogels beads in the presence of two disease biomarkers. To increase the rate of degradation of the hydrogel system and allow for a short time to result, the calcium alginate concentration in the beads was decreased, which negatively affected the spherical morphology of the beads. This resulted in misshapen beads and inconsistent degradation rates. We therefore hypothesized that the addition of a nonionic polymer, such as dextran, would aid in the formation of the spherical hydrogel beads without increasing time to result due to being uncharged and therefore unable to participate in the ionic crosslinking. With the introduction of the nonionic polymer dextran, we were able to reduce the calcium alginate concentration and still synthesize homogeneous spherical beads with a very simple procedure that degraded at elevated biomarker levels in the short times necessary for use at the POC.

In Chapter 2, we describe our work in optimizing our diagnostic for the detection of high levels of bicarbonate in serum as an approach for identifying metabolic alkalosis. It is a version of P. Pandolfi, H. Zhang, Y. Nadalin, M. Prasetyo, A. Toubian, B.M. Wu, and D.T. Kamei. *Degradation of Hydrogel Beads for the Detection of Serum Bicarbonate Levels for the Diagnosis of Metabolic Alkalosis at the Point of Care*, which is in preparation for submission. In Chapter 3, we modify and expand our system for the detection of high levels of phosphate in urine for aiding in the prevention of kidney disease, hyperparathyroidism, or excess vitamin D levels.

Chapter 2. Hydrogel-Based Detection of High Levels of Bicarbonate in Serum

2-1 Introduction

A hydrogel is a three-dimensional network of polymer chains immersed in a water-rich environment that possesses a myriad of physicochemical properties which allow for versatile applications in many areas of research.[10] In bioengineering, current research explores the application of hydrogels to tissue regeneration,[11] cell encapsulation,[12–14] biofabrication,[15] drug delivery,[16] biosensing,[17]and diagnostics.[18] Notable examples of hydrogel diagnostic applications include incorporation of hydrogels with lateral-flow immunoassays for the detection of SARS-CoV-2,[18] multifunctional colorimetric monitoring of pH and glucose levels in chronic wounds in diabetic patients,[19] and hydrogel-based microfluidic assays for the rapid detection of biomarkers that delay wound healing.[20] Another example is the application of hydrogels for bacterial detection through chemical modification of the hydrogel components with colorimetric substrates. In this study, enzymes specific to different bacteria strains catalyzed cleavage reactions that induced the release of colorimetric markers for visual detection of the specific strains by the naked eye.[17] However, all of these methods introduced many complexities to the synthesis of the hydrogel system due to the need for chemically modifying the hydrogel components in order to create a matrix with specificity towards the biomarker of interest.[17–20] Nevertheless, inspired by the application of hydrogels that produce simple, easy to read colorimetric results, we designed a diagnostic with easily interpretable results that uses hydrogels that require minimal labor and inexpensive reagents and equipment to synthesize.

A commonly used hydrogel-forming polymer is alginate, which exhibits low toxicity, high biocompatibility, low cost, and innate gelation properties.[21]Alginate is a naturally occurring

polysaccharide co-polymer that is composed of (1,4)-linked β-d-mannuronate and α-l-guluronate blocks in varying compositions and sequences [22] One notable property of alginate is its ability to bind to divalent cations through the process of ionic crosslinking in order to form hydrogels.[23] Ionic crosslinking is a spontaneous process that occurs due to electrostatic attractive interactions between positively charged divalent cations such as calcium and the negatively charged carboxyl functional groups in the alginate polymer chains. This interaction between calcium and alginate will result in an intricately woven network of the alginate polymer forming a calcium alginate gel.[23] Notably, this reaction is reversible as the calcium alginate gel network can be disassembled in response to various external stimuli such as the introduction of a metal chelator, which can be advantageous for use in many applications.[24] The disassembling of the gel network could cause the release of encapsulated dye molecules, resulting in a more robust visual output that can be easily interpreted by untrained personnel at the point of care (POC). Thus, calcium alginate gels have the potential for use in POC settings like mobile clinics due to their ease of synthesis, versatility, low cost, ability to retain dye for visual colorimetric detection, and their sensitivity towards external stimuli.

Our research focuses on the development of a POC device for the detection of metabolic alkalosis. Metabolic alkalosis results from the disruption of the acid-base equilibrium in the body, and is commonly related to kidney disease, hyperparathyroidism, and excess vitamin D levels. In metabolic alkalosis, there is either a net accumulation of base or a loss of acid in the blood often caused by chloride ion depletion from excessive vomiting, diuretic abuse, starvation, or chloride deficient diets, many of which are common in hospital patients. Consequently, a surplus of bicarbonate ions are present in the body which can lead to an elevated physiological pH, compromising cell and organ functions.[25] Normal serum levels of bicarbonate range from a

concentration of 22 to 29 mmol/L. Samples with serum bicarbonate concentrations of 30-40 mmol/L are indicative of alkalosis, yet most patients fail to present immediate symptoms. In severe alkalosis cases, serum bicarbonate concentrations can range from 40 to 50 mmol/L, causing patients to experience various levels of hypoxemia. Above 50 mmol/L, the patient is at great risk for seizures, altered mental states, and coma. Severe cases of metabolic alkalosis that present significantly elevated blood pH have 45-80% mortality rates, highlighting the importance of early disease detection.[26] Current gold standard diagnostics require expensive lab equipment that require significant power, trained personnel, and a long time-to-result. Additionally, these tests are limited to measuring pH and arterial blood gasses, such as dissolved oxygen and carbon dioxide, to indirectly calculate the serum bicarbonate concentration. Thus, there is a need to develop a rapid and efficient diagnostic to detect bicarbonate levels for early-stage metabolic alkalosis so that blood pH can be restored to safe levels in a timely manner. This work introduces such a device through utilizing the physicochemical degradation properties of calcium alginate dextran (CaAD) hydrogel beads for the detection of metabolic alkalosis at the POC.

The detection assay takes advantage of the reaction between bicarbonate and citric acid to form citrate, a strong metal chelator. The resultant reaction between citrate and calcium in the hydrogel will result in the degradation of the hydrogel beads, allowing for simple disease detection by the naked eye. Degradation rates of the hydrogel beads could therefore be directly correlated with bicarbonate concentration. However, conventional calcium alginate beads made with simple procedures would take a long time to degrade at even elevated levels of serum bicarbonate due to the high levels of calcium that would need to be chelated away from the hydrogel. In order to increase the rate of degradation and allow for a rapid time to result, the calcium alginate concentration in the beads was decreased, but this negatively affected the spherical morphology of

the beads, resulting in misshapen beads and inconsistent degradation rates. We therefore hypothesized that the addition of a nonionic polymer, such as dextran, would aid in the formation of the spherical hydrogel beads without increasing time to result due to being uncharged and therefore unable to participate in the ionic crosslinking. With the introduction of the nonionic polymer dextran, we were able to reduce the calcium alginate concentration and still synthesize homogeneous spherical beads with a very simple procedure that degraded at elevated bicarbonate levels in the short times necessary for use at the POC.

2.2 Materials and Methods

2.2.1 Preparation of the polymer solution and gelation bath

All reagents and materials were purchased from Sigma-Aldrich (St. Louis, MO) unless otherwise noted. To synthesize calcium alginate hydrogel beads, a 1% w/w sodium alginate solution was first prepared in deionized water. Additionally, 0.25 mg of Coomassie Brilliant Blue G-250 dye (Fisher Scientific, Hampton, NH) in deionized water was added per 1 mL of polymer solution for hydrogel visualization. To observe the effects of different nonionic polymers on the ionic crosslinking mechanism and the overall hydrogel properties, polymer solutions were also prepared with 1% w/w sodium alginate and 20% w/w additional polymer in deionized water. The additional polymers tested had various molecular weights of dextran, polyethylene glycol (PEG), and ethylene oxide-ran-propylene oxide (EOPO). For the salt gelation bath, a 1% w/w calcium chloride solution was prepared in deionized water. To study bead morphology and dye retention properties at lower calcium alginate percentages, 0.4, 0.6, and 0.8% w/w sodium alginate solutions with either 20, 30, 40, or 50% w/w dextran 6k were prepared. For these trials, the gelation baths were made with 0.4, 0.6, and 0.8% w/w calcium chloride in deionized water, respectively.

2.2.2 Hydrogel synthesis

The simple experimental setup we employed for synthesizing the hydrogel beads is shown in Figure 2-1. A 1 mL Luer lock syringe (VWR, Radnor, PA) containing the polymer solution was positioned vertically with its attached 30G needle tip (Thomas Scientific, Swedesboro, NJ), and suspended approximately 10 cm above a glass scintillation vial (Fisher Scientific, Hampton, NH) containing the gelation bath. The syringe needed to be a certain height above the scintillation vial to ensure that the emulsion droplets would hit the continuous phase at a speed fast enough to allow for full droplet immersion in the gelation bath. This was to ensure uniform crosslinking during hydrogel formation to generate beads of the desired spherical geometry. The syringe plunger was gently pressed to continuously dispense polymer droplets. After the polymer solution was fully dispensed, the hydrogel beads were left to incubate in the gelation bath at room temperature for at least 1 h to allow for completion of the crosslinking reaction, further stabilizing the hydrogel matrix. After the incubation period, the hydrogel beads were collected and washed with deionized water to remove excess calcium chloride ions. To examine the morphologies and dye release properties of different hydrogel beads, 20 beads of each type were stored in 3 mL of deionized water in a scintillation vial. Pictures were taken in a controlled lighting environment with an iPhone 12 camera (Apple, Cupertino, CA) immediately after placement in water, as well as after 8 days of incubation.

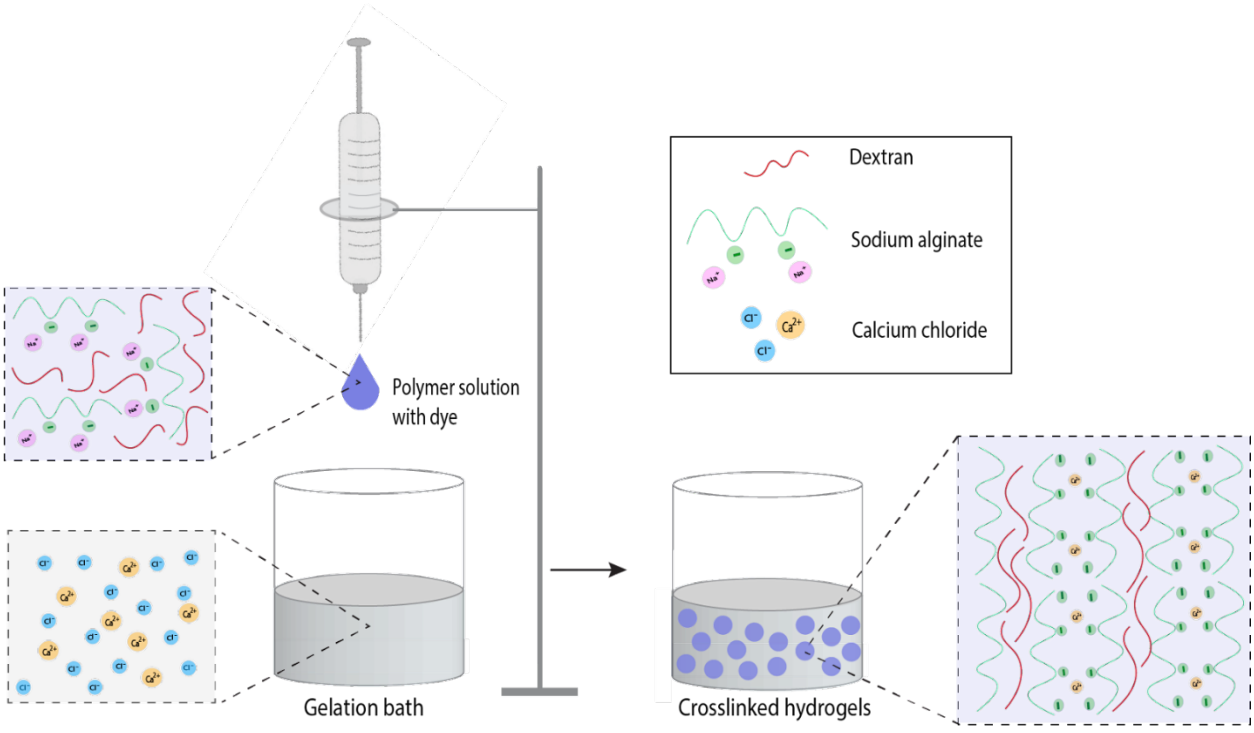

Figure 2-1. Schematic of the ionic crosslinking set up for CaAD hydrogel bead synthesis. Briefly, the polymer solution containing sodium alginate and dextran is dispensed dropwise into the gelation bath containing calcium chloride, allowing for the complexation between alginate polymers and calcium ions to form a spherical gel matrix instantaneously.

2.2.3 Degradation properties of hydrogel beads

Degradation rates of CaAD hydrogel beads in the presence of bicarbonate, citric acid, and citrate were studied separately. Ten 1% calcium alginate/20% dextran 6k beads were incubated in 2 mL microcentrifuge tubes (VWR, Radnor, PA) containing either 1.5 mL of 50 mmol/L sodium bicarbonate in phosphate-buffered saline (PBS) (Gibco, Waltham, MA), 1.5 mL of 50 mmol/L citric acid in PBS, or 1.5 mL of 50 mmol/L sodium citrate in PBS. Additionally, 10 beads were incubated in PBS without sodium bicarbonate as a negative control. All tubes were placed on a nutator mixer (Clay Adams, New York, NY) at 12 RPM at room temperature. Pictures were taken with an iPhone 12 camera when the degradation reaction was initiated (t=0 min), and each time significant degradation of hydrogel beads was observed.

2.2.4 Detection of bicarbonate

The detection of bicarbonate concentrations was carried out as follows for all hydrogel bead formulations and sample environments. Eight 2 mL microcentrifuge tubes were prepared with 1.485 mL of PBS or human serum (lot # 502036415, Fisher Scientific, Hampton, NH) spiked with varying concentrations of sodium bicarbonate (0, 20, 25, 30, 35, 40, 45 and 50 mmol/L). Next, 15 µL of citric acid in PBS at a concentration of 1 g/mL was added into each tube. 10 hydrogel beads were then transferred into each tube to start the degradation reaction. The tubes were placed on a nutator at 12 RPM at room temperature. Pictures of all tubes were taken with an iPhone 12 camera immediately after the degradation reaction started (t=0 min) and each time complete hydrogel bead degradation was observed.

2.2.5 Development of the POC Device

All parts were designed in Autodesk Fusion 360 and sliced in Ultimaker Cura. Parts were printed using the 3D printer Ultimaker 3 (Utrecht, Netherlands). Structural components were printed using copolyester filament and joints were printed using thermoplastic polyurethane. The device was designed to house a DC 6V 10 RPM motor (Walfront, Lewes, DE) powered by a battery pack containing 4 AA batteries connected in a simple circuit. Due to the applied load, the resulting rotational speed of the motor was estimated to be 9 RPM. The motor was used to rotate a 2 mL microcentrifuge tube and its housing about its horizontal axis. The rotational speed of the device was further adjusted with the use of a 2:1 gear system to increase the RPM to a desired value of approximately 18.

2.3. Results and Discussion

2.3.1 Hydrogel bead morphology studies

As shown in Figure 2-2A, 1% calcium alginate hydrogel beads synthesized without an additional nonionic polymer were neither spherical nor uniform in size. In order to develop a robust diagnostics assay that depends on bead degradation rates, it was essential to find a hydrogel bead formulation that consistently yielded uniform and spherical beads. For this reason, we introduced an additional nonionic polymer component to the alginate solution when synthesizing the hydrogel beads. Interestingly, all of the hydrogel beads synthesized with 1% calcium alginate and 20% nonionic polymer showed better morphologies overall, demonstrated by their spherical shapes. More specifically, PEG 4.6k, PEG 20k, and dextran 6k beads showed the best morphologies in terms of monodispersity and spherical geometry. On the other hand, while EOPO and dextran 35-45k beads were uniform and appeared spherical from the top view (Figure 2-2A), they were flatter and appeared disk-like when observed from the side view (Figure 2-2B). This was unfavorable because disc-shaped beads are more difficult to visualize from the side and hold less dye than a spherical bead, hindering the visual detection of degradation. It is currently unclear why the addition of a second polymer improves bead morphology. Presumably, the change in viscosity and/or surface tension of the polymer solution could be factors, but further studies are necessary to confirm this possibility.

2.3.2 Stability and dye retention

To develop a diagnostic assay with a long shelf-life, it is necessary for the hydrogel beads to be both stable in water and capable of retaining dye for an extended period of time. Therefore, the stability and dye release properties of the hydrogel beads were studied over time. As shown in

Figure 2-2B, all hydrogel beads retained their original morphologies in deionized water over 8 days indicating good stability. Dye release, demonstrated by the increase in blue dye in the water, demonstrated that hydrogel beads containing the nonionic dextran 6k had the best dye retention. For all other hydrogel beads, there was an increase of dye in water visible to the naked eye after 8 days. More specifically, PEG 4.6k and dextran 35-45k beads exhibited slight release, followed by greater release from EOPO 12k beads, and the most release from PEG 20k beads. As a result, dextran 6k was selected as the nonionic polymer to be added to the alginate solution for hydrogel bead synthesis.

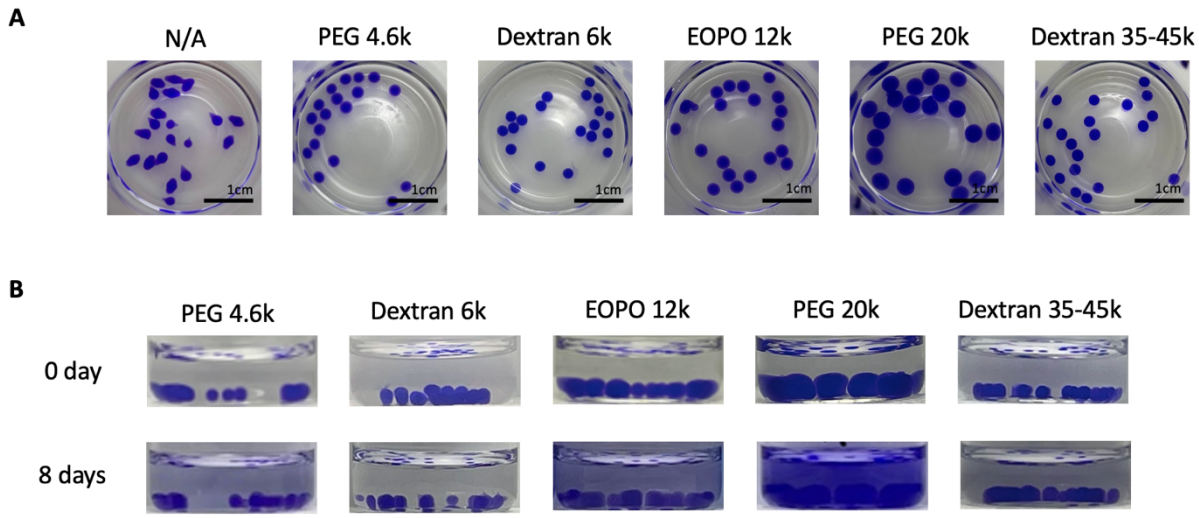

Figure 2-2. Morphology and release behavior of 1% calcium alginate hydrogel beads synthesized with and without an additional nonionic polymer in the polymer solution. A. Overall morphology of the different hydrogel compositions. The leftmost hydrogel beads contained no additional polymer, while the others (from left to right) contained 20% PEG 4.6k, 20% dextran 6k, 20% EOPO 12k, 20% PEG 20k, and 20% dextran 35-45k. **B**. Dye release study. From left to right, the beads were made with 20% PEG 4.6k, 20% dextran 6k, 20% EOPO 12k, 20% PEG 20k, and 20% dextran 35-45k.

2.3.3 Dextran hydrogel bead degradation studies

While the hydrogel beads were shown to have good stability in water, calcium alginate gels are also known to be responsive to various external stimuli. One such example is the gel-sol

transition response of the calcium alginate in the presence of certain metal chelators as well as enzymes such as alginate ligase.[27–29] In this assay, the degradation properties of the hydrogels assisted by calcium chelators were utilized to achieve the visual detection of high levels of bicarbonate. Specifically, calcium chelators degrade the gel matrix by binding to the divalent calcium cations that are crosslinked with alginate, thereby disrupting the gel matrix and causing bead degradation to occur. Some common calcium chelators used for calcium alginate gel degradation are ethylenediamine tetraacetic acid (EDTA), ethylene glycol tetraacetic acid (EGTA), 1,2-bis(o-aminophenoxy)ethane-N,N,N',N'-tetraacetic acid (BAPTA), and citrate.[29,30] Interestingly, bicarbonate, the biomarker of metabolic alkalosis, also has the ability to bind to calcium to form calcium bicarbonate complexes. However, its binding activity was shown to be weak in comparison to citrate, exemplified by the slower degradation rate of the hydrogel beads with 1% calcium alginate and 20% dextran 6k in 50 mmol/L bicarbonate at 50 min compared with their fast degradation rate in 50 mmol/L citrate at 7 min as shown in Figure 2-3. The slow degradation rate of the hydrogel beads due to the bicarbonate is not ideal for the POC detection of metabolic alkalosis, which requires a rapid result. Therefore, in order to speed up degradation of dextran hydrogel beads by bicarbonate, excess citric acid was added to samples containing bicarbonate to yield citrate via the following reaction.

$$3NaHCO_3 + C_6H_8O_7 \rightarrow 3Na^+ + C_6H_5O_7^{3-} + 3H_2O + 3CO_2$$

As a control, we also examined the degradation of hydrogel beads with 1% calcium alginate and 20% dextran 6k in 50 mmol/L citric acid, and as also shown in Figure 2-3, citric acid by itself did not degrade the hydrogel beads over a 5 h period. Therefore, when using citric acid, the degradation rates of the hydrogel beads can be solely attributed to the formation of citrate, whose amount is

directly correlated to the concentration of bicarbonate present in the patient's serum sample through the above reaction.

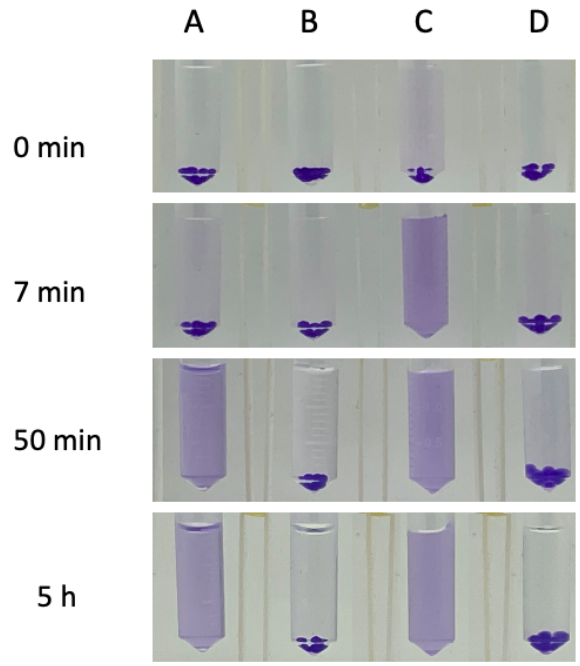

Figure 2-3. Degradation properties of hydrogel beads with 1% calcium alginate and 20% dextran 6k in sodium bicarbonate, citric acid, and sodium citrate. **A.** Hydrogel degradation in 50 mmol/L sodium bicarbonate in PBS. **B.** Hydrogel degradation in 50 mmol/L citric acid in PBS. **C.** Hydrogel degradation in 50 mmol/L sodium citrate in PBS. **D.** Hydrogel degradation in PBS.

2.3.4 Detection of bicarbonate in PBS

After separately testing the degradation properties of hydrogel beads with 1% calcium alginate and 20% dextran 6k in bicarbonate, citric acid, and citrate, their degradation due to the bicarbonate-citric acid reaction was observed. Eight concentrations of sodium bicarbonate in PBS with an excess of citric acid were chosen to model varying concentrations of bicarbonate; concentrations below 30 mmol/L indicate the absence of metabolic alkalosis, concentrations at 30 mmol/L and above correspond to abnormal bicarbonate levels indicating metabolic alkalosis, and 0 mmol/L was the negative control. Figure 2-4 shows that degradation of the hydrogel beads was only observed in bicarbonate concentrations at 35 mmol/L and above. Specifically, the hydrogel

beads in 50 mmol/L bicarbonate completely degraded in 37 min, followed by complete degradation in 45 mmol/L bicarbonate at 1 h 10 min. Complete degradation in 40 mmol/L bicarbonate only occurred at 11 h 35 min, and complete degradation of the hydrogel beads was not observed for bicarbonate concentrations of 35 mmol/L or below after 11 h. This trend proves that the degradation rates of the hydrogel beads can be directly correlated to the concentration of bicarbonate in PBS. However, the current degradation times were not yet ideal for POC diagnostics due to the long time-to-result for bicarbonate concentrations between 35 and 45 mmol/L.

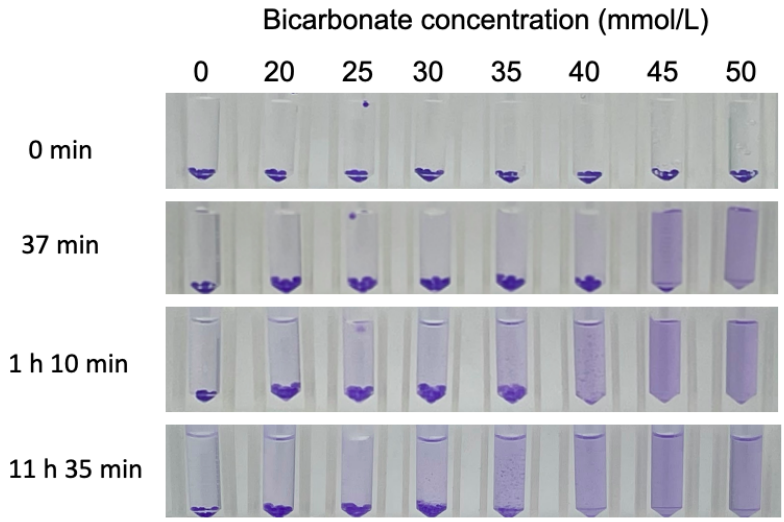

Figure 2-4. Degradation properties of hydrogel beads with 1% calcium alginate and 20% dextran 6k in varying concentrations of bicarbonate in PBS. From left to right the concentrations of bicarbonate are 0, 20, 25, 30, 35, 40, 45, and 50 mmol/L.

2.3.5 Gel bead optimization for the detection of bicarbonate

In order to design a rapid diagnostic assay, the degradation rates of the hydrogel beads needed to be accelerated. This was achieved by further lowering the percentage of calcium alginate in the gel beads. Faster degradation occurred with the lower calcium concentrations in the gel structure, since less citrate was required to completely chelate calcium cations and disassemble the gel matrix. However, hydrogels with a lower calcium alginate concentration exhibit less uniform

bead morphology. For this reason, the concentration of dextran in the polymer solution was increased accordingly (20%, 30% and 40%) while keeping the sodium alginate concentration constant (Figure 2-5A). Hydrogel beads with 1% calcium alginate and 50% dextran were not able to be synthesized due to the high viscosity of the polymer solution. For 0.2% and 0.4% calcium alginate hydrogel beads, significant increases in dextran concentrations showed little visible improvement in bead morphology. In contrast, hydrogel beads with 0.6% and 0.8% calcium alginate and 40% dextran concentrations showed notable improvement in size and uniformity. Therefore, the degradation properties of hydrogel beads with 0.6% and 0.8% calcium alginate and 40% dextran were tested in varying levels of bicarbonate in PBS, as shown in Figures 2-5B and 2-5C, respectively. For hydrogel beads with 0.6% calcium alginate and 40% dextran, complete degradation was not observed for 0 and 20 mmol/L bicarbonate. For 25, 30, and 35 mmol/L bicarbonate, full degradation was observed at 3 h, 1 h 24 min, 26 min, and 23 min, respectively. Lastly, degradation occurred at 14 min for both 45 and 50 mmol/L bicarbonate concentrations. For hydrogel beads with 0.8% calcium alginate and 40% dextran, complete degradation was not observed for 0, 20, and 25 mmol/L bicarbonate. Bicarbonate concentrations of 30, 35, 40, and 45 mmol/L showed complete degradation at 5 h 30 min, 2 h 4 min, 1 h 24 min, and 19 min, respectively. For both systems with 40% dextran, the degradation rates of the hydrogel beads substantially increased in comparison to hydrogel beads with 1% calcium alginate and 20% dextran (Figure 2-4). In addition, it was observed that both hydrogel bead systems with 40% dextran in elevated levels of bicarbonate from 35 mmol/L to 50 mmol/L showed much faster degradation rates compared to the concentrations close to or lower than the cut-off value typically used for metabolic alkalosis diagnosis, 30 mmol/L. This notable finding allows for rapid and easy visual confirmation of the presence of elevated bicarbonate concentrations in a sample.

Furthermore, since the hydrogel beads with 0.6% calcium alginate exhibited faster degradation properties than 0.8% calcium alginate, while maintaining good stability and morphology, these beads were further investigated. The stability and dye retention studies of hydrogel beads with 0.6% calcium alginate and 40% dextran 6k can be found in Figure 2-6.

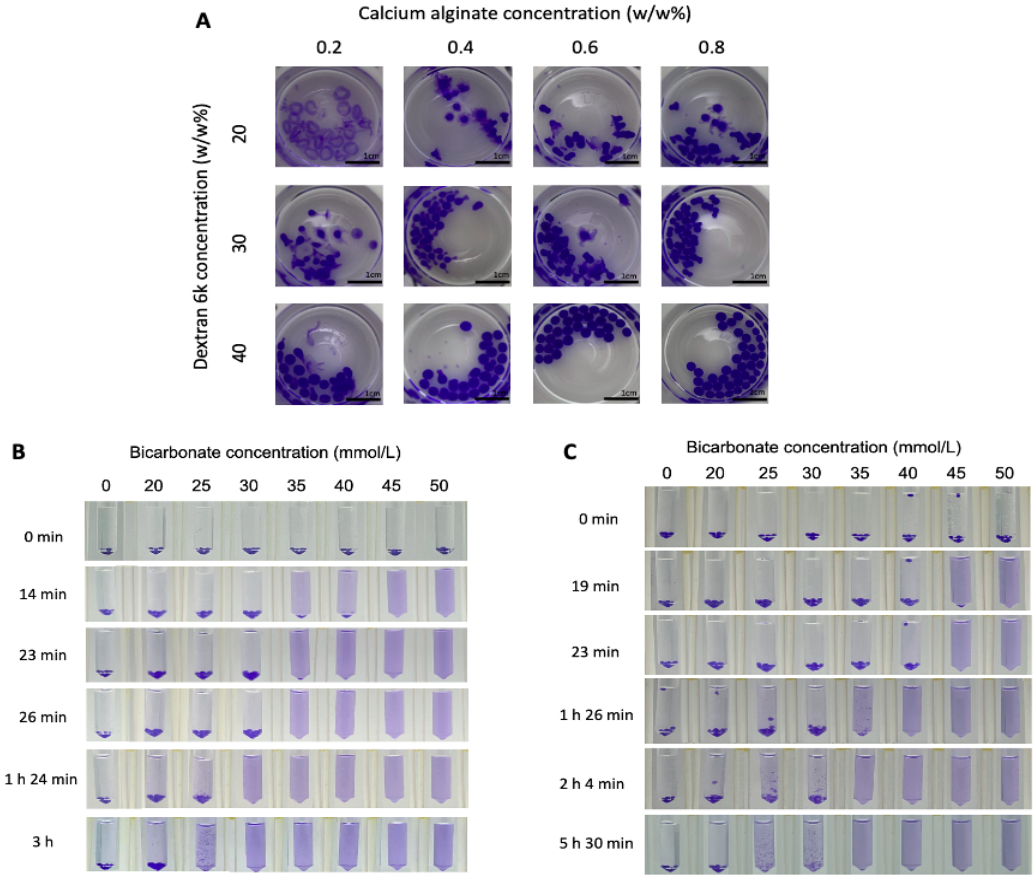

Figure 2-5. Optimization of CaAD hydrogel beads for the detection of abnormal concentrations of bicarbonate. A. Synthesis of CaAD hydrogel beads with varying calcium alginate and dextran 6k concentrations to optimize bead morphology for faster degradation rates. **B.** Degradation of hydrogel beads with 0.6% calcium alginate and 40% dextran 6k in varying concentrations of bicarbonate (0, 20, 25, 30, 35, 40, 45, and 50 mmol/L) in PBS over time. **C.** Degradation of hydrogel beads with 0.8% calcium alginate and 40% dextran 6k in varying concentrations of bicarbonate (0, 20, 25, 30, 35, 40, 45, and 50 mmol/L) in PBS over time.

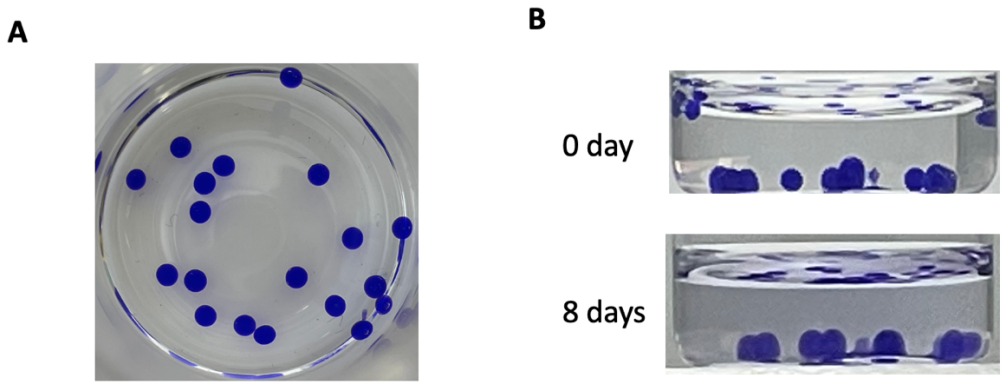

Figure 2-6. Stability and dye retention studies of hydrogel beads with 0.6% calcium alginate and 40% dextran 6k. A. Morphology of 0.6% calcium alginate and 40% dextran 6k **B.** Stability and dye release study

2.3.6 Detection of bicarbonate in human serum

After achieving desirable degradation rates of the hydrogel beads with 0.6% calcium alginate and 40% dextran 6k in varying levels of bicarbonate in PBS, identical trials from Figure 2-5B were carried out using human serum samples spiked with bicarbonate to verify if our POC diagnostics could function similarly in serum. As shown in Figure 2-7, the CaAD hydrogel beads at 50 mmol/L degrade completely in 10 min, followed by complete degradation in bicarbonate concentrations of 45, 40 and 35 mmol/L at 15 min, 20 min, and 54 min, respectively. The hydrogel beads in the lower bicarbonate concentrations of 30 and 25 mmol/L completely degraded in 2 h 12 min and 3 h 36 min, respectively. Lastly, the CaAD hydrogel beads in 0 and 20 mmol/L did not show significant degradation for 3 h 36 min. This degradation trend in human serum follows Figure 2-4C closely. Specifically, the degradation times of the CaAD hydrogel beads in the highest 3 bicarbonate concentrations were similar to those obtained in PBS. Moreover, although the degradation in 35 mmol/L bicarbonate was slowed down by half an hour relative to the PBS case, it remained within the assay's one hour time frame. The degradation times in 30 and 25 mmol/L

bicarbonate were also slower in comparison to the experiments in PBS (Figure 2-5B). These slight decreases in degradation times could potentially be attributed to inhibitors present in human serum. As the degradation rates of CaAD hydrogel beads in bicarbonate concentrations of 30 mmol/L and below were much slower than the degradation rates in the abnormal bicarbonate concentrations of 35 mmol/L and above, this system can be used to accurately detect for most elevated bicarbonate levels in human serum ranging from 35 mmol/L to 50 mmol/L indicated by the fast degradation of the CaAD hydrogel beads and the release of the blue dye.

Overall, the degradation times of the CaAD hydrogel beads were successfully reproduced in human serum and proved to be well suited for diagnosis at the POC. The assay will be interpreted as follows: complete degradation of the CaAD hydrogel beads under one hour indicates abnormal concentrations of bicarbonate (35 mmol/L and above) in serum suggesting a high possibility of the patient exhibiting metabolic alkalosis. At critically high concentrations of bicarbonate, the CaAD beads degrade in 20 min or less. In contrast, no significant degradation of the CaAD hydrogel beads occurred after an hour for serum levels of bicarbonate that are normal or near the cut-off value for metabolic alkalosis (30 mmol/L and below).

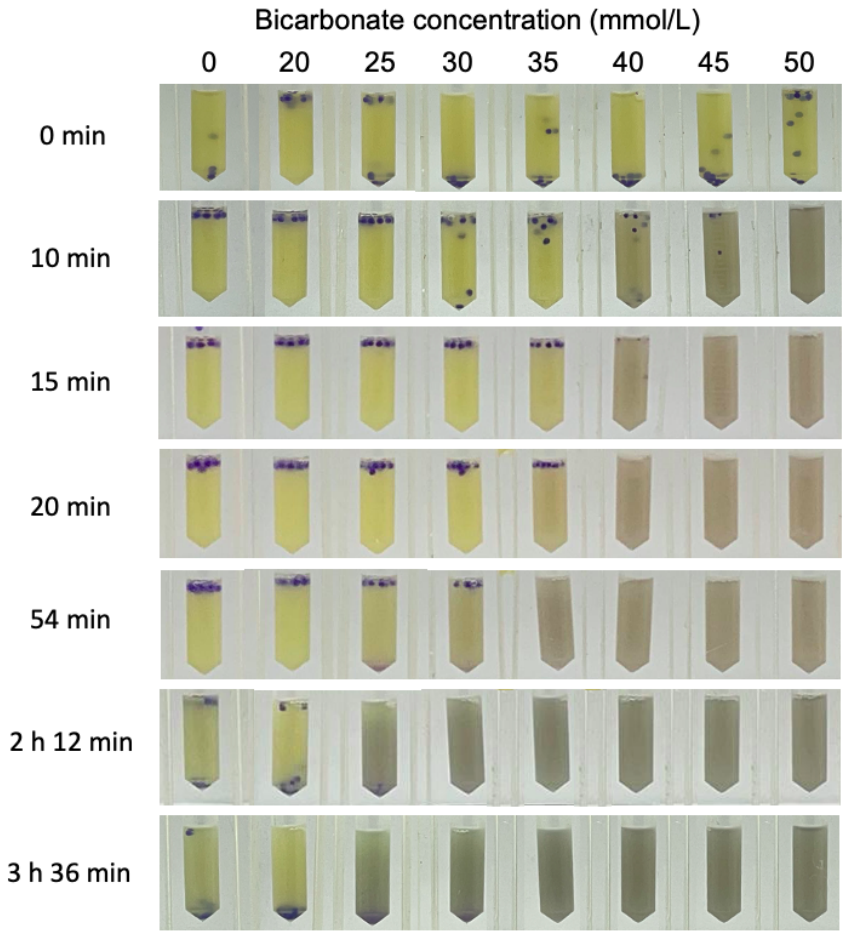

Figure 2-7. Degradation of hydrogel beads with 0.6% calcium alginate and 40% dextran 6k in varying concentrations of bicarbonate in human serum. From left to right the concentrations of bicarbonate are 0, 20, 25, 30, 35, 40, 45, and 50 mmol/L.

2.3.7 Device for the point of care

A POC-friendly device (Figure 2-8) was developed to aid in the detection of metabolic alkalosis in replacement of the lab equipment nutator. This device will be suitable for use in mobile clinics and resource-limited areas due to its small size, portability, low cost, low power requirements, and ease of use.

To test if the previous results attained in the nutator can be replicated with our device, degradation of hydrogel beads in 0, 30, 40, and 50 mmol/L bicarbonate in human serum were observed by placing the microcentrifuge tubes containing the CaAD hydrogel beads in the device.

As shown in Figure 2-9, the hydrogel beads degraded at 10 min, 23 min, and 1 h 40 min in 50, 40, and 30 mmol/L bicarbonate samples, respectively. The CaAD hydrogel beads in the negative control (0 mmol/L bicarbonate) did not exhibit degradation within 6 h. These degradation times were close to those attained with the nutator (10 min, 20 min, and 2 h 12 min for 50, 40, and 30 mmol/L bicarbonate concentrations, respectively). These findings validate the efficacy of the device for use in the rapid detection of metabolic alkalosis at the POC.

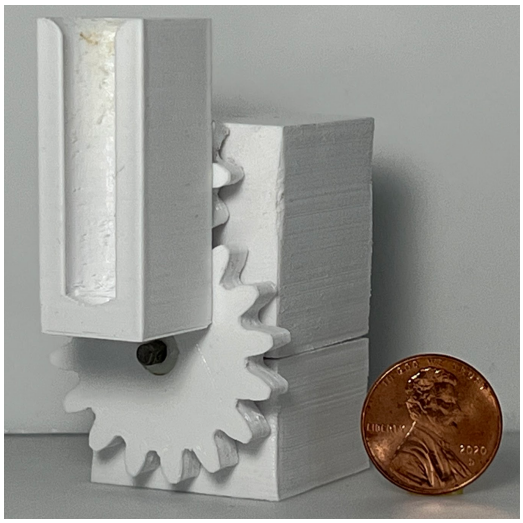

Figure 2-8. Device for the detection of metabolic alkalosis at the POC. A microcentrifuge tube holder is attached to a rotating motor powered by a battery pack. A US penny is included for size comparison.

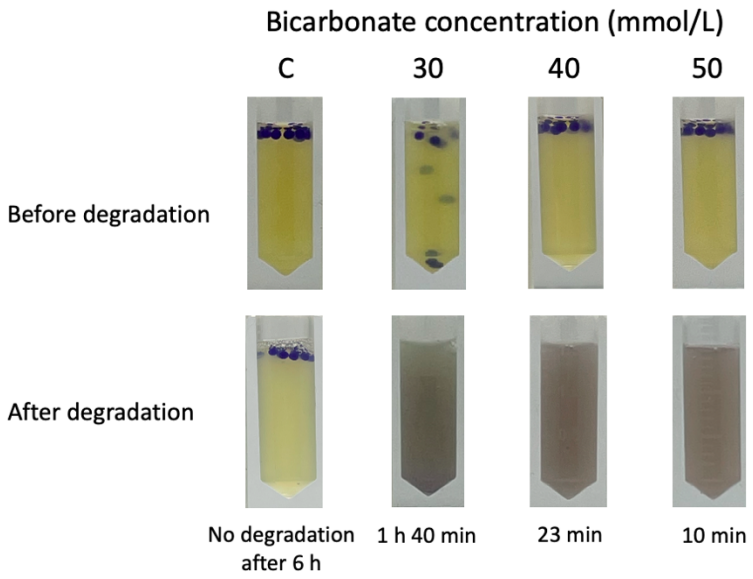

Figure 2-9. Degradation of hydrogel beads with 0.6% calcium alginate and 40% dextran 6k in varying bicarbonate concentrations in human serum using the POC diagnostic device. From left to right the concentrations of bicarbonate are 0, 30, 40 and 50 mmol/L.

2.4. Conclusion

We successfully developed a POC diagnostic assay using novel hydrogel beads for the detection of metabolic alkalosis. To our knowledge, we are the first group to study and apply CaAD hydrogel beads for diagnostics. Specifically, optimized hydrogel beads with 0.6% calcium alginate and 40% dextran 6k showed excellent properties for rapid detection of high concentrations of bicarbonate in both PBS and serum samples. The detection step involves the reaction of excess citric acid with bicarbonate, a marker for metabolic alkalosis functioning as the limiting reagent to produce citrate. Citrate, a strong calcium chelator, rapidly disassembles the CaAD gels, and the degradation time was correlated with bicarbonate concentrations in serum. Our device effectively detects high bicarbonate concentrations of 35 mmol/L and above, which indicates metabolic alkalosis, in less than an hour. More specifically, a serum bicarbonate concentration of 50 mmol/L was detected in as little as 10 min. Additionally, sodium bicarbonate concentrations of 45, 40, and

35 mmol/L were detected in 15, 20, and 54 min, respectively. In contrast, CaAD hydrogel beads in bicarbonate concentrations near the cut-off value of metabolic alkalosis (30 mmol/L and below) require well above an hour to show signs of degradation. Similar results were attained with our developed POC device. Thus, our inexpensive, rapid, and simple assay has the potential to be used in mobile clinics for the detection of metabolic alkalosis at the POC.

Chapter 3: Hydrogel-Based Detection of High Levels of Phosphate in Urine

3.1 Introduction

Phosphate is the negatively charged form of phosphorus, which is a mineral that is found throughout the body and is mostly stored in the bones and teeth in the form of calcium phosphate.[31] High levels of phosphate may be caused by kidney disease, hyperparathyroidism, or excess vitamin D, while low levels are a symptom of hypoparathyroidism, hypercalcemia, liver or kidney disease, or severe malnutrition.[32] Thus, monitoring phosphate levels can aid in the early detection of these conditions. The monitoring of phosphate levels is typically performed in serum, which requires a blood extraction step as well as sample preparation and detection performed in a laboratory. Such an approach might take up to 1-2 days for results in addition to requiring expensive equipment and trained personnel.[33] Accordingly, there is a need to develop a rapid and inexpensive device that can measure phosphate levels directly in urine to yield results on-site for patients who are at risk for a disease. In a healthy adult, normal levels of phosphate found in urine are 0.4-1.3 grams in a 24-h period.[34] It is important to note that the average adult excretes varying amounts of urine a day ranging from 0.8-2 L which is determined by the type and the volume of the ingested fluids as well as the person's kidney function.[35] For this preliminary study, the phosphate concentrations tested were based on a person excreting 0.8 L of urine a day. Thus, we set out to detect abnormally high levels of phosphate, higher than 1.3 grams per day, with our hydrogel system presented in Chapter 2. Specifically, we took advantage of the reaction between phosphate and calcium to form calcium phosphate. In theory, high concentrations of phosphate will successfully outcompete alginate and bind to calcium ions present in the gel matrix. This will result in gel degradation, which will be indicative of the presence of our biomarker.

3.2 Materials and Methods

3.2.1 Preparation of polymer solution

All reagents and materials were purchased from Sigma-Aldrich (St. Louis, MO) unless otherwise noted. To synthesize CaAD hydrogel beads, 0.6 and 0.8% w/w sodium alginate solutions with 40% w/w dextran 6k were first prepared in deionized water. Additionally, 0.25 mg of Coomassie Brilliant Blue G-250 dye (Fisher Scientific, Hampton, NH) in deionized water was added per 1 mL of polymer solution for easy hydrogel visualization. The gelation bath was composed of 0.6 and 0.8% w/w calcium chloride.

3.2.2 Hydrogel synthesis

The simple experimental setup we employed for synthesizing the hydrogel beads is shown in Figure 2-1. A 1 mL Luer lock syringe (VWR, Radnor, PA) containing the polymer solution was positioned vertically with its attached 30G needle tip (Thomas Scientific, Swedesboro, NJ), and suspended approximately 10 cm above a glass scintillation vial (Fisher Scientific, Hampton, NH) containing the gelation bath. The syringe needed to be a certain height above the scintillation vial to ensure that the droplets would hit the gelation bath at a speed fast enough to allow for full droplet immersion in the gelation bath. This was to ensure uniform crosslinking during hydrogel formation to generate beads of the desired spherical geometry. The syringe plunger was gently pressed to continuously dispense polymer droplets. After the polymer solution was fully dispensed, the hydrogel beads were left to incubate in the gelation bath at room temperature for at least 1 h to allow for completion of the crosslinking reaction, further stabilizing the hydrogel matrix. After the incubation period, the hydrogel beads were collected and washed with deionized water to remove excess calcium chloride ions.

3.2.3 Detection of phosphate in urine

Hydrogel beads with 0.8% calcium alginate and 40% dextran 6k were synthesized to test for phosphate-triggered degradation. The gels were incubated for 1 h in the gelation bath to allow for the continuation of the crosslinking reaction between alginate and calcium to form stable hydrogels. Potassium phosphate monobasic was used to spike solutions with the appropriate concentration of phosphate ions. Briefly, 1.5 mL solutions of 0, 1, 1.5, 1.6, 1.625, 1.7, 1.8, 1.9, 2, and 2.5 mg/mL of phosphate were made in synthetic urine in 2 mL microcentrifuge tubes. 3 gel beads were placed in each tube, and all the trials were placed in the nutator at room temperature. Hydrogel degradation was subsequently monitored over time.

3.2.4 Detection of phosphate in urine with the optimized hydrogel formulation

Hydrogel beads with 0.6% calcium alginate and 40% dextran 6k were synthesized to test for phosphate-triggered degradation. After their synthesis, the gels were incubated for 1 h in the gelation bath to allow for the continuation of the crosslinking reaction between alginate and calcium to form stable hydrogels. Briefly, solutions of 0, 1, 1.6, 1.8, 2, and 2.5 mg/mL of phosphate were made in synthetic urine in 2 mL microcentrifuge tubes. 3 gel beads were placed in each tube, and all of the trials were placed in the nutator at room temperature. Hydrogel degradation was subsequently monitored over time.

3.2.5 Device at the point of care

All parts were designed in Autodesk Fusion 360 and sliced in Ultimaker Cura. Parts were printed using the 3D printer Ultimaker 3 (Utrecht, Netherlands). Structural components were printed using copolyester filament, and joints were printed using thermoplastic polyurethane. The

device was designed to house a DC 6V 10 RPM motor (Walfront, Lewes, DE) powered by a battery pack containing 4 AA batteries connected in a simple circuit. Due to the applied load, the resulting rotational speed of the motor was estimated to be 9 RPM. The motor was used to rotate a 2 mL microcentrifuge tube and its housing about its horizontal axis. The rotational speed of the device was further adjusted with the use of a 2:1 gear system to increase the RPM to a desired value of approximately 18.

3.3 Results and Discussion

3.3.1 Detection of phosphate in urine

Hydrogel beads with 0.8% calcium alginate and 40% dextran 6k were synthesized as shown in Figure 3-1A. Our proposed assay depends on the mechanism of phosphate competing with alginate for the binding of calcium cations as phosphate can react with calcium to form calcium phosphate. In this way, the timeframe for gel bead degradation should be directly correlated to the phosphate ion concentration in the sample. Figure 3-1B shows that this gel bead formulation did not exhibit the desired degradation trend in relation to phosphate levels. This is exemplified in the trials with 1.6, 1.625, 1.7, and 2 mg/mL of phosphate, where there was complete degradation of the gel beads after 47 min for all of these concentrations. Additionally, the 0, 1, 1.5, 1.8, 1.9, and 2.5 mg/mL phosphate concentrations were all not fully degraded at 47 min. This is concerning not only because there is no trend that correlates phosphate levels to hydrogel degradation but also because many of the concentrations dissolved at the same rate as the control, which has no phosphate. This indicated that the gel beads in this assay were mostly degraded by unknown components in the synthetic urine solution.

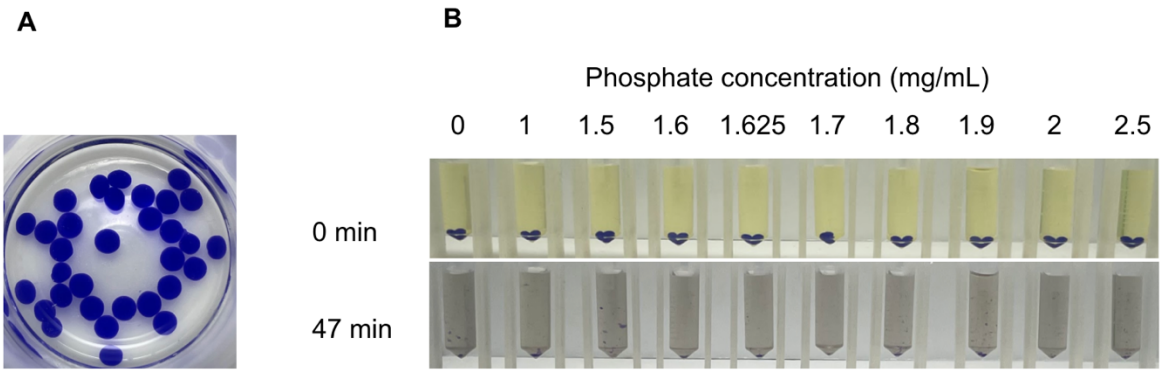

Figure 3-1. Morphology and phosphate-induced degradation of 0.8% calcium alginate/40% dextran 6k hydrogels in synthetic urine. A. Morphology of hydrogel beads. **B.** From left to right, solutions of 0, 1, 1.5, 1.6, 1.625, 1.7, 1.8, 1.9, 2, and 2.5 mg/mL of phosphate were made in synthetic urine, and 3 gel beads were added to each solution.

3.3.2 Detection of phosphate in urine with the optimized hydrogel formulation

Hydrogel beads with 0.6% calcium alginate and 40% dextran 6k were synthesized as shown in Figure 3-2A. A lower concentration of calcium alginate was selected because we wanted to speed up the phosphate-induced gel bead degradation. We reasoned that accelerating the degradation rate could generate a trend that correlated degradation time with phosphate levels, minimizing the effects of other synthetic urine components on degradation time. Figure 3-2B demonstrates that we were able to generate a trend of gel bead degradation time with phosphate levels in urine. Specifically, 2.5, 2, 1.8, 1.6, and 1 mg/mL of phosphate degraded the beads in 20, 23, 24, 25, and 25 min, respectively, while the control (0 mg/mL of phosphate) degraded the beads in 31 min. Considering healthy and non-healthy levels of phosphate, the assay exhibited a 5-min time window between the degradation of a critically high phosphate level, 2.5 mg/mL, and healthy concentrations, which are lower than 1.6 mg/mL. Further optimizations are therefore necessary to increase this window of time from 5 min.

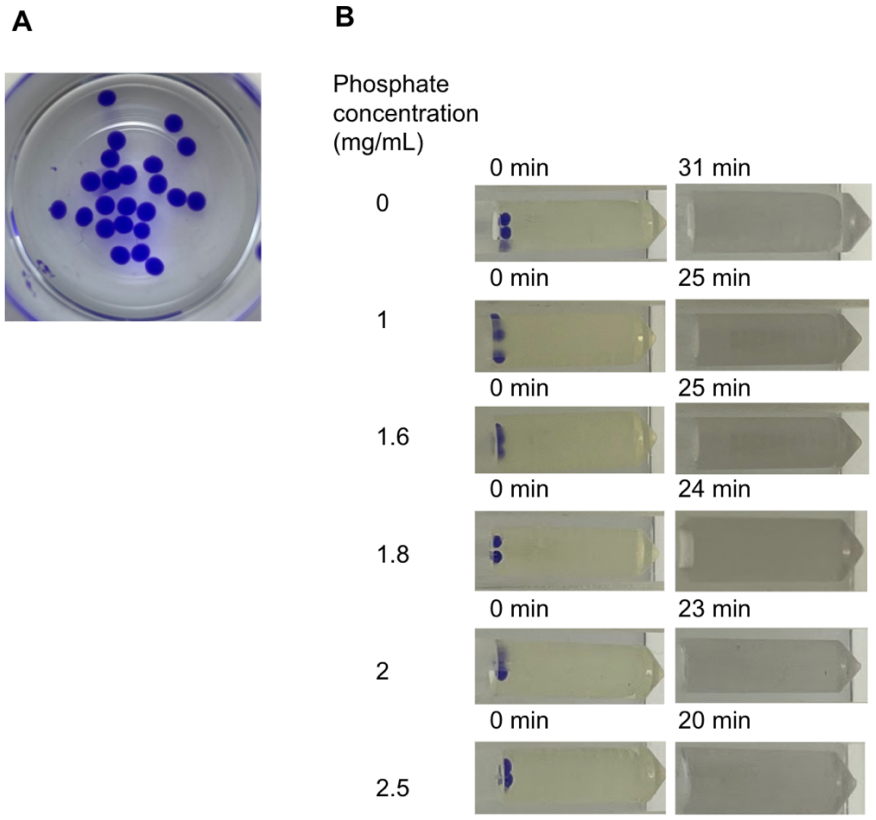

Figure 3-2. Morphology and phosphate-induced degradation of 0.6% calcium alginate/40% dextran 6k hydrogels in synthetic urine. **A.** Morphology of hydrogel beads. **B.** From left to right, solutions of 0, 1, 1.6, 1.8, 2, and 2.5 mg/mL of phosphate were made in synthetic urine, and 3 gel beads were added to each solution.

3.3.3 Detection of phosphate in urine with the POC device

In this assay, the nutator was replaced with a POC device that incorporated a 360° microcentrifuge tube rotation. Solutions of 0, 1.6, 1.7, 1.8, and 2 mg/mL of phosphate were made in synthetic urine to determine if this device could yield results similar to those obtained with a laboratory nutator. The device exhibited faster gel bead degradation, most likely attributed to the full inversion of the microcentrifuge tubes, in contrast to the side-to-side motion of the nutator used in past trials. The faster response is advantageous especially since the results from the device could be similarly correlated with phosphate concentrations (comparing Figure 3-3B with Figure

3-2B). Specifically, 2, 1.8, 1.7, and 1.6 mg/mL of phosphate degraded the beads in 15, 16, 17, and 18 min, respectively, while the control (0 mg/mL) degraded the beads in 19 min. As in the case of using the nutator, further optimizations are necessary as the differences in degradation times should be increased.

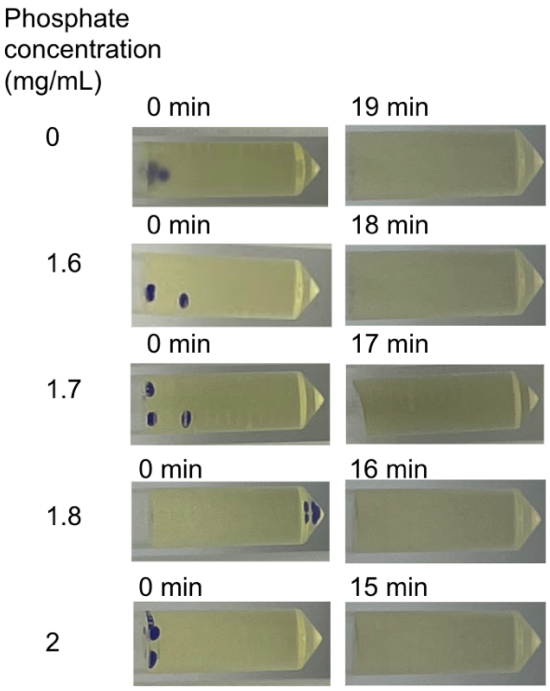

Figure 3-3. Phosphate-induced degradation of 0.6% calcium alginate/40% dextran 6k hydrogels in synthetic urine with the POC device. From left to right, solutions of 0, 1.6, 1.7, 1.8, and 2 mg/mL of phosphate were made in synthetic urine, and 3 gel beads were added to each solution.

3.4 Conclusion

A POC system for the detection of high concentrations of phosphate in urine was developed. The system was designed so that the user could administer the test and analyze the results on-site without the need for trained personnel or expensive equipment. Our assay was able to correlate gel bead degradation rates with phosphate concentrations. The diagnostic device would only need a small volume of sample from each patient to deliver the results in as little as 16 min,

as the system detects for critically high urine phosphate concentrations of 2 mg/mL and 1.8 mg/mL in 15 min and 16 min, respectively. On the other hand, the cut-off for normal urine phosphate levels, 1.6 mg/mL, fully degraded in 18 min.

The small window of time between the complete degradation of normal and abnormal phosphate levels is undesirable and should be addressed in future work to avoid potential misdiagnosis. This could be achieved by decreasing the magnitude of the mechanical stress introduced to the assay, such as by lowering the device RPM as well as by not employing 360^{o} rotation, to achieve overall slower gel bead degradation. Moreover, the diagnostic could also be optimized to successfully detect phosphate concentrations in patients excreting 2 L of urine daily since this work focused on the lower end of 0.8 L of urine being excreted daily. The phosphate concentrations would be even lower for a greater volume of urine, and detection of these lower phosphate concentrations may be achieved by further lowering the calcium alginate concentration as well as investigating other external stimuli to which the hydrogel is extremely sensitive.

References

1 K. Chaturvedi, K. Ganguly, U. A. More, K. R. Reddy, T. Dugge, B. Naik, T. M. Aminabhavi and M. N. Noolvi, *Natural Polysaccharides in Drug Delivery and Biomedical Applications*, 2019, 59–100.

2 V. V. Nandini, K. V. Venkatesh and K. C. Nair, *Journal of Conservative Dentistry: JCD*, 2008, **11**, 37.

3 ALGINATE FIBRES – AN OVERVIEW - Fibre2Fashion, https://www.fibre2fashion.com/industry-article/591/alginate-fibres-an-overview, (accessed May 12, 2022).

4 R. G. Puscaselu, A. Lobiuc, M. Dimian and M. Covasa, *Polymers (Basel)*, 2020, **12**, 1–30.

5 P. Sofia, P. Batista, A. Maria, M. Bernardo De Morais, M. Manuela, E. Pintado and R. M. Santos Costa De Morais, 2019, 649–691.

6 Alginic acid, aluminum hydroxide, and magnesium carbonate Uses, Side Effects & Warnings - Drugs.com, https://www.drugs.com/mtm/alginic-acid-aluminum-hydroxide-and-magnesium-carbonate.html, (accessed April 20, 2022).

7 L. Li, Y. Fang, R. Vreeker, I. Appelqvist and E. Mendes, DOI:10.1021/bm060550a.

8 Y. Qin, *Polymer International Polym Int*, 2008, **57**, 171–180.

9 F. Abasalizadeh, S. V. Moghaddam, E. Alizadeh, E. akbari, E. Kashani, S. M. B. Fazljou, M. Torbati and A. Akbarzadeh, *Journal of Biological Engineering*, 2020, **14**, 8.

10 Y. S. Zhang and A. Khademhosseini, *Science (1979)*, DOI:10.1126/SCIENCE.AAF3627/ASSET/DA9C967B-F098-46FD-8612-68D9054A7DF3/ASSETS/GRAPHIC/356_AAF3627_FA.JPEG.

11 R. A. Stile and K. E. Healy, *Biomacromolecules*, 2001, **2**, 185–194.

12 O. W. Petersen, L. Ronnov-Jessen, A. R. Howlett and M. J. Bissell, *Proc Natl Acad Sci U S A*, 1992, **89**, 9064.

13 F. Chowdhury, Y. Li, Y. C. Poh, T. Yokohama-Tamaki, N. Wang and T. S. Tanaka, *PLOS ONE*, 2010, **5**, e15655.

14 S. R. Caliari and J. A. Burdick, *Nature Publishing Group*, 2016, **13**, 405.

15 B. J. Klotz, D. Gawlitta, A. J. W. P. Rosenberg, J. Malda and F. P. W. Melchels, *Trends in Biotechnology*, 2016, **34**, 394–407.

16 Y. Qiu and K. Park, *Advanced Drug Delivery Reviews*, 2001, **53**, 321–339.

17 Z. Jia, M. Müller, T. le Gall, M. Riool, M. Müller, S. A. J. Zaat, T. Montier and H. Schönherr, *Bioactive Materials*, 2021, **6**, 4286–4300.

18 R. A. Barclay, I. Akhrymuk, A. Patnaik, V. Callahan, C. Lehman, P. Andersen, R. Barbero, S. Barksdale, R. Dunlap, D. Goldfarb, T. Jones-Roe, R. Kelly, B. Kim, S. Miao, A. Munns, D. Munns, S. Patel, E. Porter, R. Ramsey, S. Sahoo, O. Swahn, J. Warsh, K. Kehn-Hall and & B. Lepene, , DOI:10.1038/s41598-020-78771-8.

19 Y. Zhu, J. Zhang, J. Song, J. Yang, Z. Du, W. Zhao, H. Guo, C. Wen, Q. Li, X. Sui and L. Zhang, *Advanced Functional Materials*, 2020, **30**, 1905493.

20 D. Puchberger-Enengl, C. Krutzler, F. Keplinger and M. J. Vellekoop, *Lab on a Chip*, 2013, **14**, 378–383.

21 K. Y. Lee and D. J. Mooney, *Prog Polym Sci*, 2012, **37**, 106.

22 F. Alihosseini, *Antimicrobial Textiles*, 2016, 155–195.

23 M. A. Abd El-Ghaffar, M. S. Hashem, M. K. El-Awady and A. M. Rabie, *Carbohydrate Polymers*, 2012, **89**, 667–675.

24 M. Kobašlija and T. McQuade, *Biomacromolecules*, 2006, **7**, 2357–2361.

25 A. S. Hoffman, *Journal of Controlled Release*, 1987, **6**, 297–305.

26 S. Tripathy, *Indian Journal of Critical Care Medicine: Peer-reviewed, Official Publication of Indian Society of Critical Care Medicine*, 2009, **13**, 217.

27 R. Diryak, M. H. Kontogiorgos, M. Vassilis, G. Smith, Alan M and A. Uk, .

28 B. Doumèche, J. Picard and V. Larreta-Garde, *Biomacromolecules*, 2007, **8**, 3613–3618.

29 S. J. Dixon, K. M. Lemberg, M. R. Lamprecht, R. Skouta, E. M. Zaitsev, C. E. Gleason, D. N. Patel, A. J. Bauer, A. M. Cantley, W. S. Yang, B. Morrison and B. R. Stockwell, *Cell*, 2012, **149**, 1060–1072.

30 E. Keowmaneechai and D. J. McClements, *Journal of Agricultural and Food Chemistry*, 2002, **50**, 7145–7153.

31 Definition of phosphate - NCI Dictionary of Cancer Terms - NCI, https://www.cancer.gov/publications/dictionaries/cancer-terms/def/phosphate, (accessed May 12, 2022).

32 Phosphate in Urine - Results, https://wa.kaiserpermanente.org/kbase/topic.jhtml?docId=hw202342#hw202372, (accessed April 21, 2022).

33 Phosphate in Blood: MedlinePlus Medical Test, https://medlineplus.gov/lab-tests/phosphate-in-blood/, (accessed May 12, 2022).

34 Phosphate in Urine - Test Overview, https://wa.kaiserpermanente.org/kbase/topic.jhtml?docId=hw202342, (accessed May 12, 2022).

35 Excessive Urination Volume (Polyuria), https://www.healthline.com/health/urination-excessive-volume#other-causes, (accessed May 8, 2022).